2016 23rd Iranian Conference on Biomedical Engineering and 2016 1st International Iranian Conference on Biomedical Engineering (ICBME), Amirkabir University of Technology, Tehran, Iran, 23-25 November 2016

A General Algorithm for Automatic Lesion Segmentation in Dermoscopy Images

Neda Zamani Tajeddin, Babak Mohammadzadeh Asl
Dept. of Biomedical Engineering
Tarbiat Modares University
Tehran, Iran
{n.zamanitajeddin, babakmasl} @ modares.ac.ir

***Abstract*—Melanoma is one of the most dangerous types of skin cancer and causes thousands of deaths worldwide each year. Recently dermoscopic imaging systems have been widely used as a diagnostic tool for melanoma detection. The first step in the automatic analysis of dermoscopy images is the lesion segmentation. In this article, a novel method for skin lesion segmentation that could be applied to a variety of images with different properties and deficiencies is proposed. After a multi-step preprocessing phase (hair removal, illumination correction, etc.), a robust histogram-based thresholding technique is used to obtain an initial mask of the lesion. The initial mask is used to sample the lesion's color and drive a contour propagation algorithm. A color probability map of the image is calculated based on sampled pixels and Bayesian classification. Using this probability map and image gradient, a novel dual-component speed function is constructed to improve the performance of propagation model. The proposed algorithm has been tested on the ISIC dataset of 900 dermoscopy images, and gained high values for evaluation metrics e.g. Dice and Jaccard coefficient values of 0.89 and 0.79, respectively. Also, the proposed algorithm ranked 5th in the ISBI melanoma segmentation challenge.**

Keywords-melanoma; segmentation; thresholding; level sets; contour propagation; ISBI melanoma challenge.

I. INTRODUCTION

Skin cancer-related death cases are increasing in all parts of the word, with over than 9000 deaths each year [1]. Melanoma, which is the most dangerous type of skin cancer, is a major public health problem. So it is very important to diagnose the melanoma as early as possible. In order to diagnose skin lesions, dermatologists at first step use dermoscopy, which has a magnify glass with polarization filter and a uniform light. Dermoscopy is a noninvasive diagnostic tool that makes the subsurface areas of skin more visible and it helps to reveal more details from lesion features such as dot/globules, streaks, and pigment networks [2].

Because of early detection and non-invasive diagnosis to avoid unnecessary biopsy, computer aided diagnostic (CAD) methods are very popular. The CAD provides algorithms for automatic processing of skin lesions. Generally, these methods consist of three steps: 1) border detection which is called lesion segmentation, 2) feature extraction and 3) classification [3].

The first step in the skin lesion image analysis is to detect the lesion border from the other regions of skin. A variety of methods has been proposed in the literature to achieve this aim [4]. The most used segmentation methods can be categorized into threshold based [5, 6], edge based [8, 9], region based [4, 10], color clustering and active model based algorithms [9]. Among this algorithms, thresholding techniques are very popular due to their automatic and straight implementation. Despite their simplicity, thresholding methods would not always lead to a perfect result, especially when deficiencies exist in image or lesion has a weak appearance in some regions. For more comprehensive reviews on dermoscopy image segmentation techniques refer to [2, 9, 10].

Our goal in this article is to introduce a general method for lesion segmentation in dermoscopic images. There is several drawbacks in designing such a general algorithm. These problems originated from the fact that most of the dermoscopic images are defected with noise, hairs, dark corners, color charts, uneven illumination, marker ink, etc. So far, the other researchers in the literature tested their algorithms on limited datasets, in which all the images have similar specifications. In real terms, dermoscopy image datasets are more complicated. They may have different properties for each image and all kind of disturbance may exist, like the dataset we working on. A general framework for segmentation should be capable of overcoming these difficulties. Preprocessing is a way to handle most of these deficiencies. Therefore, in this work, we will discuss an extensive field of preprocessing tasks to improve the image quality and facilitate the segmentation procedures. Then, in order to automate the segmentation procedure, a histogram-based threshold is used to obtain an initial mask of the lesion. This initial mask may not contain all the lesion regions in the image, especially in multi-colored lesions. So, a novel method based on color information and contour propagation is proposed. A block diagram of proposed segmentation method can be seen in Fig. 1.

Rest of the paper is arranged as follow: in section II the methodology of proposed method is explained in details. This section consists of two main phases itself. In section III, the experimental results of applying the proposed method on the available dataset are presented qualitatively and quantitatively. And finally, the paper is concluded in section IV.

978-1-5090-3452-9/16/$31.00 ©2016 IEEE

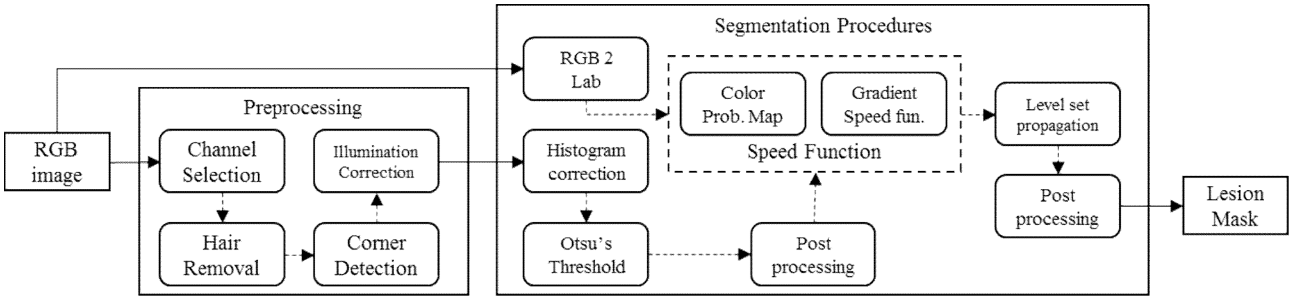

Figure 1: Overview of proposed segmentation algorithm.

II. METHODS

As block diagram of Fig. 1 displays, the algorithm designed for lesion border detection is comprised of two main different parts. Each of these parts is described in the fallowing sections.

A. Preprocessing

The preprocessing procedure has several tasks or steps. Each of which has been designed to eliminate the effect of particular deficiency in the image. Since further operations are based on a single-channel gray-level image, the first step in the preprocessing must be the color to gray-level image conversion. This task could be simply done by selecting Blue channel of RGB color space or can be done using more sophisticated approaches to selected/construct the optimal color channel. Here, based on [9] we compare the entropy of different channels to select a most entropic channel, $I(x, y)$. From here, all operations are based on this selected channel, unless otherwise be told. There are several works proposing different approaches for preprocessing [2, 9, 10]. According to the available dataset, we select or design the most appropriate algorithms for different task as follow:

Hairs and ruler marks inpainting: Presence of hairs in some dermoscopic images could make the segmentation process more difficult. Even with a fair lesion segmentation, in further steps of image analysis, like feature extraction and classification, the hairs may confuse the results. So it is recommended to remove the hairs from the image before any further processing. In this article, we use the well-known DullRazor filter [10] to remove the hairs from the image. DullRazor performs the following steps:

1. It identifies the dark hair locations by a generalized grayscale morphological closing operation,
2. It verifies the shape of the hair pixels as thin and long structure, and replace the verified pixels by a bilinear interpolation, and
3. It smoothes out the replaced hair pixels with an adaptive median filter.

DullRazor is not the most state-of-the-art algorithm for hair in painting, but it just performs well for our application. With this approach ruler marks will be removed from the image as well because they have similar thin long structures as hairs.

Dark corner detection: Some cases in the dataset show a dark and shadowy circular (rectangular sometimes) pattern in corners of the image. In some cases these dark regions cover more than half of image area (Fig. 2.a), hence, pixel values corresponding to these regions would be dominant in the histogram of the image and this fact would cause error in calculating the threshold (making an initial mask). Ergo, we design a new algorithm to obtain the corner mask and compensate for it in further processes.

To obtain the initial corner mask, we used a constant threshold for Y channel of CMYK color system, because this channel represents the Black color in the image and has a good discriminant between the dark corner and other parts of the image. In some cases, the lesion is also dark and is enough big to reach the corners, so they will be identified as corner mask as well. To prevent this from happening, in a novel and yet simple approach, we consider a set of predefined masks for the corners. These predefined masks would limit the obtained border mask using the thresholding technique. In our approach, selecting the appropriate mask from the set of predefined masks is carried out based on pixels information in nine different regions of the image. The mean pixel intensity from these regions is captured and compared to a reference to decide whether that region is located in the dark corner or not. Based on the different configuration of all nine regions, the most appropriate predefined (limiting) mask is selected. Finally, the corner mask is constructed by applying logical AND operation to the initial corner mask and predefined mask.

Illumination Correction: Uneven illumination in the image add complexity to the histogram and can lead to a wrong threshold selection. There are several approaches proposed for illumination correction. Some approaches are based on illumination model captured from a wide range of training images, these methods are not applicable to the dermoscopy images because the lesions in different images have different sizes and appearances. So, it is hard to obtain a single illumination model for background in a general dataset of dermoscopy images. The other group of illumination correction approaches obtain the illumination model or correct the illumination based on a single image information.

We use homomorphic filtering [11] for this part of preprocessing, it simultaneously normalizes the brightness across an image and increases the contrast. The homomorphic filter is an old but yet efficient and stand-alone technique to correct for non-uniform illumination. These methods assume a multiplicative noise model for image, in which the object reflectance R is the signal we interested in and scene illumination L is the noise to be filtered:

$$I(x, y) = L(x, y)R(x, y) \quad (1)$$

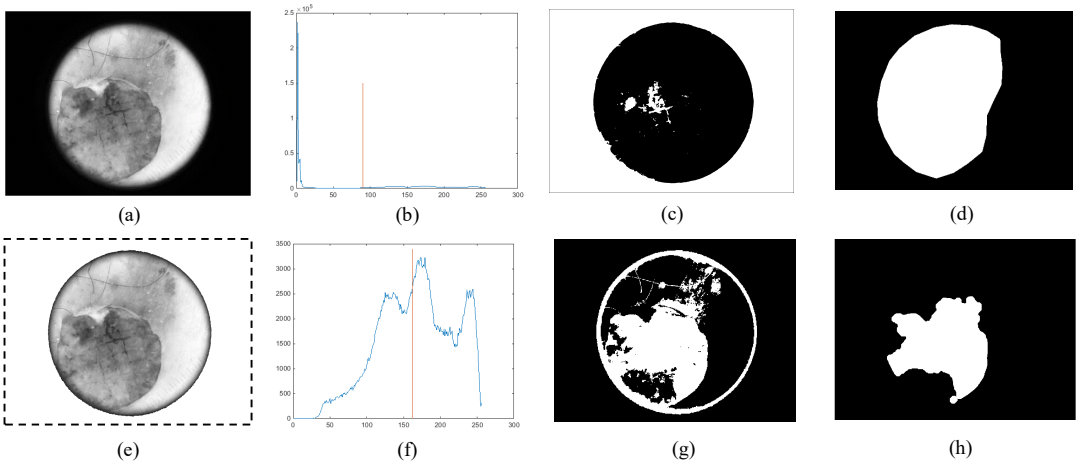

Figure 2: Effect of correcting the histogram counts on selecting the optimal threshold: (a) is original gray-level image, (b) is corresponding histogram of (a) and calculated threshold (red line), (c) is binary mask based on threshold in (b), (e) is masked image with the corner mask, (f) is corrected histogram of the masked image and it's threshold (red line), (g) is binary mask obtained with threshold calculated based on (f), (h) is post processed binary mask in (h), and (d) displays the ground truth segmentation.

To compensate for the non-uniform illumination, the key is to remove the illumination component L and keep only the reflectance component R . Illumination typically varies slowly across the image as compared to reflectance which can change quite abruptly at object edges. This difference is the key to separating out the illumination component from the reflectance component. In homomorphic filtering, we first transform the multiplicative components to additive components by moving to the log domain:

$$\begin{aligned} \ln\left(I(x,y)\right) &= \ln\left(L(x,y)\,R(x,y)\right) \\ \ln\left(I(x,y)\right) &= \ln\left(L(x,y)\right) + \ln\left(R(x,y)\right) \end{aligned}, \qquad (2)$$

then we use a high-pass filter in the log domain to remove the low-frequency illumination component while preserving the high-frequency reflectance component [11].

B. Segmentation Process

In this article, we use deformable models for melanoma segmentation. Usually, these approaches start from an initial condition and evolve through iterations to finally converge. Some of the deformable models use edge (gradient) information to deform the initial curve to the boundary of the desired object in the image i.e. Snakes and Geodesic Active Contour (GAC), some other use regional information for contour evolution, like Chan-Vese method [9].

We use level sets to represent the contour. This type of contour representation has been taken into consideration in many medical image applications. We use the level set approach introduced by Malladi et al. [12] in a novel framework to propagate an initial contour toward the lesion boundary. In addition to image gradient information, here we use image color information to form the speed function. So, our approach would benefit from both gradient and region information. This property makes the algorithm robust against weak edges and faded color regions. To be able to capture the correct color information of the desired region to form the speed function and also initializing the model contour, we need a primary mask of the lesion in the image. This binary mask is obtained using Otsu's thresholding technique [13]. This binary mask is processed and its contour extracted to be used in further operations. The fallowing paragraphs express the details of segmentation procedure:

1) Initial mask through thresholding

In the current work, the binary mask of the lesion is obtained using Otsu's methods [13]. Among tested thresholding techniques [6], Otsu's method works the best on our dataset. Otsu's approach is a histogram based thresholding method that tries to select an optimal threshold that partition the histogram into two classes. Selected threshold must minimize intra-class variance (the variance within the class). If we have an image histogram ($p(i); i = 0,\ldots,l-1$) with l different gray-levels, Otsu's method select the optimal threshold, t_{Otsu} , as follow:

$$t_{\text{Otsu}} = \arg\min_{t} \left\{ \sigma_0^2(t) \left(\sum_{i=0}^{t-1} p(\text{i}) \right) + \sigma_1^2(t) \left(\sum_{i=t}^{l-1} p(\text{i}) \right) \right\} \qquad (3)$$

In the above equation, threshold t separates the histogram into two classes, $\sigma_0^2(t)$ and $\sigma_1^2(t)$ are variances of these two classes. The calculated optimal threshold can be used to convert the gray-level image into a binary mask.

In some cases, the area of pixels that occupied by dark corners or color charts is comparable to lesion area or even whole image area. Therefore, this deficiency (dark corner or charts) would contribute a great deal in histogram bins and this fact will affect the thresholding technique performance. As displayed in Fig. 2.a~c this effect would lead to wrong results.

We employed a new trick to correct the histogram before employing the Otsu's method. As we obtained the corner mask in preprocessing steps, we can use this mask to compensate for dark corner effect in the histogram. To correct the histogram, we first masked the image with obtained corner mask (set the image pixels corresponded to corner mask equal to 1, Fig. 2.e) and then calculate the histogram of masked image. We count

the pixels that belong to the corner (chart) regions in the corner mask and then subtract the count from the last element of the histogram. In this way, we eliminate the effect of dark corners in the histogram, hence, the corrected histogram contains only the information related to lesion and skin pixels (Fig. 2.f). This is a simple and yet very effective technique that have never been used in other researches. Fig 2.g shows the result of implying Otsu's method on the corrected histogram. As you can see correcting the histogram plays a significant rule in calculating the optimal threshold.

The primary binary mask does not represent an ideal segmentation of the lesion and it is not appropriate to be used as the initial mask of active contour because it has many noises and outside lesion objects. So we implement some post-processing task on the primary binary mask to make it more suitable for further operations. This post-processing generally contains morphological operations, like closing, opening, hole-filling, area filtering and border cleaning. In Fig. 2.h results of implementing these operations on the binary mask obtained from the previous section are depicted. From here on, we mention this processed mask as an *initial mask*.

2) Modeling the lesion color

A very challenging issue in designing of an automatic lesion segmentation algorithm, which could be generalized to a variety of lesions, is handling the images with weak gradient magnitude i.e. images with weak edges and strokes. Unfortunately, most of the model-based segmentation algorithms employ edge information and are not appropriate for this situation. We propose to somehow engage the color information as well to handle this kind of problem. For this end, we need to model the color information of some lesion's pixels and then use this model to classify all the pixels in the image. In this way, we can obtain a probability map of each pixel contribution to the lesion.

In this work, we capture the color information from L*a*b* color space because unlike the RGB space, a* and b* color information are independent of the lightening condition in the image. So, for each pixel in the image, we sample the value of a* and b* in a vector as color information of that pixel. We use the color information of the pixels that are related to the region specified by the initial mask to estimate the parameters of the color probability distribution of the lesion. Therefore, we classify the pair of (a*,b*) of each pixel in the image, using Bayesian classification over the estimated color probability distribution, in order to obtain a probability map of color information in image. Please note that the color information is independent of edge or gradient information. So, this is a binary classification problem and we assume equal prior probability for both classes. Also, we consider the maximum likelihood (ML) of the data (D) which is the most probable hypothesis (H) i.e. $F_{\mathrm{c}} = ML \equiv \arg\max_{h \in H} \{\mathrm{P}(D \mid h)\}$ as the color probability map.

3) The propagation model

As we mentioned before, the initial mask obtained by thresholding is not an ideal segmentation of the lesion. Our goal in this subsection is to use the information in the initial mask region to evolve this initial boundary until it contains all the lesion. We realize this evolving process through the level set framework based on the work of Malladi et al. [12].

The initial curve is extracted from the boundary of the initial mask. Malladi's method propagates this closed curve with a speed of F in its normal direction. They use the implicit representation of the curve i.e. the level set approach is used to embed the curve in a higher-dimensional function $\psi(x,t)$ so that the initial curve would be the zero level set of that function $\psi(x,t=0)$ [13]. We consider the signed distance function (SDF) of the initial mask as the level set function. There is some advantages in using the level set approach for this kind of problems that are fully discussed in [12, 14].

Malladi et al. proposed a partial differential equation for the evaluation of ψ as follow:

$$\psi_t + F|\nabla\psi| = 0, \qquad \psi(x,t=0) \text{ given} \tag{4}$$

This is a recursive formulation that can be used to iteratively update the ψ function. In every update, the zero level set (evolving contour) is getting closer to the border of the lesion. In (4), F is named as *speed function* and it should be define somehow to propagate the model correctly. In the original work of Malladi et al., speed is assumed to be a decreasing function of the image gradient. A practical way to implement this definition is as follow:

$$F_{\mathrm{g}}(x,y) = \frac{1}{1+\sigma|\nabla G(x,y)|} \tag{5}$$

In the above equation, $G(x,y) = I(x,y) * g(x,y)$ is Gaussian filtered image with a standard deviation of σ, where $g(x,y) = \exp\left(-(x^2+y^2)/2\sigma^2\right) \Big/ 2\pi\sigma^2$, and * stands for convolution operation. $|\nabla G(x,y)|$ represent the magnitude of gradient function for every pixel. Gradient magnitude is normalized by multiplying it with the term σ. Based on (5), F_{g} is small where $|\nabla G(x,y)|$ is large, and is close to 1 for the regions of the image $I(x,y)$ that have a constant value.

As one can see, this speed function captures the edge (gradient) information from the image (see Fig. 3.a) and propagate the contour towards them using (4). But, as we said before in some cases the edge information are weak and are not reliable enough to drive the speed function. To address this problem, we proposed a dual-component speed function: one member of which is based on gray-level image gradient and the other one is a color probability distribution of pixels. Hence, the complete speed function, F, that has been used in (4) can be rewritten as follow:

$$F(x,y) = \alpha F_{\mathrm{g}}(x,y) + \beta F_{\mathrm{c}}(x,y) \tag{6}$$

The second term is calculated based on pixels sampled from a* and b* channels in the regions that initial mask specifies. Mean $(\mu_{\mathrm{a,b}})$ and standard deviation $(\sigma_{\mathrm{a,b}})$ of each channel samples are calculated and then a normal distribution

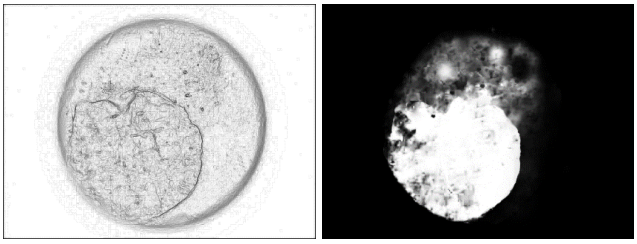

(a) (b)

Figure 3: Speed function calculated based on: (a) image gradient through (5) and (b) color probability map.

is drawn based on them. Afterward, based on this distribution all pixels of the image (a*, b*) will be classified (Fig. 3.b). Increasing the $\sigma_{a,b}$ can extend the domain of Bayesian classifier in labeling pixels as lesion. Based on our experiments 3 standard deviations of the mean can properly label the color pixels. The α and β are weights that specify the contribution of each component F_g and F_c in the construction of the final speed function, respectively.

III. Experiments and Results

In this section, we evaluate the performance of our proposed algorithm on a general multi-vendor pre-segmented dataset. The dataset that we used in this research consists of 900 dermoscopy images. These images have been selected from the International Skin Imaging Collaboration (ISIC) archive to be used as a training set in the challenge of "Skin Lesion Analysis toward Melanoma Detection" at the International Symposium on Biomedical Imaging (ISBI) 2016 [15]. The ground truth segmentation of the lesion in each image is available as well, so we can evaluate our algorithm quantitatively.

The evaluation metrics that have been used in this paper consist of two similarity coefficient and three pixel based goodness measures:

$$\begin{aligned} Dice &= 2TP/(TP+FP+TP+FN) \\ Jaccard &= TP/TP+FN+FP \\ Accuracy &= (TP+TN)/(TP+TN+FP+FN) \\ Sensitivity &= TP/(TP+FN) \\ Specificity &= TN/(TN+FP) \end{aligned} \quad (7)$$

In the above equations, TP is the number of pixels that labeled as 1 in both the segmentation output AND the ground truth, TN is the number of pixels that labeled as 0 in both the segmentation output AND the ground truth, FP is the number of the pixels that wrongly labeled as 1 in the output segmentation and FN is the number of pixels in the output that are wrongly labeled as 0. Dice and Jaccard coefficients measure the similarity between the output of segmentation algorithm and the ground truth segmentation, therefore they are appropriate to be used as segmentation evaluation metrics. All the measures in (7) return a number in the range of [0 1]. Higher metrics indicating a better segmentation performance.

Based on a validation experiment, we set the algorithm parameters as: $\sigma = 0.1, \alpha = 0.4, \beta = 0.6$. Then the proposed algorithm has been tested on all 900 images. The resulted binary masks then were compared with the expert's ground truth based on five evaluation metrics. The average of evaluation metrics on all tested images is available in Table I. As you can see the proposed method can considerably enhance the result of other algorithm.

The Dice value of 0.895 shows the reliability of our algorithm. Keep in mind that this algorithm has been tested three times on a dataset of 900 images, none of the past research has evaluated their algorithms on such an intensive dataset, quantitatively. Knowing the facts that images in the dataset are from different imaging systems and captured in different conditions and also most of them are corrupted with different deficiencies, the results of this experiment proved the generalization ability of our algorithm.

To compare the proposed algorithm with the other methods, it is necessary to apply them on this exact dataset. To our knowledge, no paper that reports its method on this specific dataset has been published yet. However, a test dataset had been published by the challenge organizers in order to compare the challenge competitors based on it. This test dataset comprises of 397 dermoscopy image without any ground truth about segmentation, with the similar difficulties as the training dataset, though. Competitors after applying their methods to this test images, submit their results in challenge website so their outputs being evaluated by five defined metrics. We don't know anything about the essence of other competitor's algorithms but based on the ranking of the challenge website, our method placed in 5th rank among 28 competitors[1] (The ranking take places based on Jaccard score). Evaluation metrics on challenge testing dataset is reported in Table II.

For the sake of qualitative evaluation of the proposed algorithm, we overlay the output contours of segmentation procedures on the original image for different cases. Six of them is displayed in Fig. 4. In these images, the green contour specifies the ground segmentation, the red contour stands for Otsu's method output and the blue contour show the border detected by our proposed algorithm. As one can see, our algorithm is very applicable even for difficult cases. In some cases with the multi-colored lesion, Otsu's method segments the dominant regions of lesion only, whilst our proposed algorithm results to a much closer border to the ground truth.

TABLE I. Results of evaluation experiment on training data

Method	Evaluation metrics (Average)				
	Dice	*Jaccard*	*Accuracy*	*Sensitivity*	*Specificity*
Maglo [8]	0.799	0.699	0.892	0728	0.981
Celebi [6]	0.813	0.721	0.907	0.726	0.988
Barata [5]	0.854	0.786	0.919	0.829	0.985
Proposed	0.895	0.802	0.935	0.832	0.987

TABLE II. Results of evaluation experiment on test data

Method	Evaluation metrics (Average)				
	Dice	*Jaccard*	*Accuracy*	*Sensitivity*	*Specificity*
Proposed[1]	0.888	0.81	0.946	0.832	0.987

[1]The challenge results are available online at (submission under the name of Neda Zamani Tajeddin):
challenge.kitware . com/#challenge/560d7856cad3a57cfde481ba.

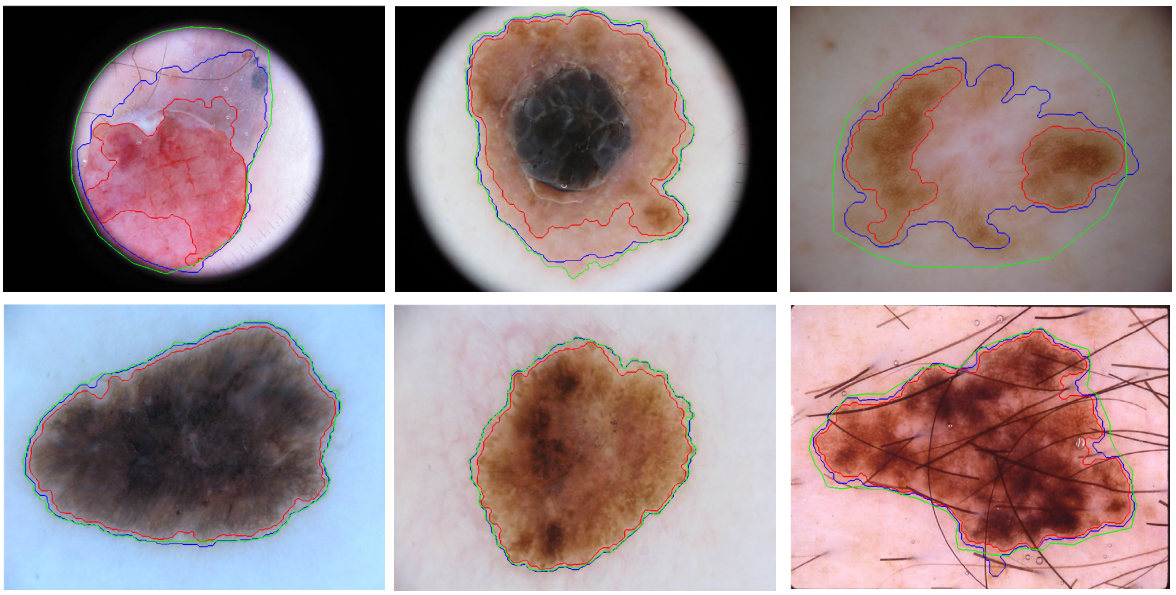

Figure 4: Six cases of melanoma image segmentation. The green contour specifies the ground segmentation, the red contour stands for Otsu's method output and the blue contour shows the border detected by our proposed algorithm.

IV. Conclusion

In this article, we proposed a general algorithm for lesion segmentation in dermoscopic images. We use several stages of preprocessing before applying the main segmentation procedure. To start the segmentation automatically, we used a novel histogram-corrected Otsu's threshold to build an initial binary mask of the lesion. The initial mask does not represent an ideal segmentation of the lesion, so a novel dual-component speed function of the image has been constructed to be used in an iterative scheme and propagate the initial contour toward the desired boundary. This new dual-component speed function makes the segmentation algorithm robust against weak gradient and faded color intensities. The evaluation experiments of the proposed method result in Dice and Jaccard coefficient values of 0.89 and 0.79, respectively. This gained high evaluation metrics and the fact that our algorithm ranked among the first 5 competitors in the international challenge of melanoma diagnosis, prove the reliability and generalizability of the proposed method.

Using more advanced methods in preprocessing phase would always lead to a more reliable segmentation. We used a full level set method in the front propagation algorithm. To further improvement in performance we suggest implementing a Fast Marching method [14] in level set framework, as well.

References

[1] B. W. Stewart and C. P. Wild, *World Cancer Report 2014*. World Health Organization, 2014.

[2] N. K. Mishra and M. E. Celebi, "An Overview of Melanoma Detection in Dermoscopy Images Using Image Processing and Machine Learning," *arXiv Prepr. arXiv1601.07843*, pp. 1–15, 2016.

[3] T. Celebi, M. Emre; Marques, Jorge S.; Mendonca, *Dermoscopy image analysis, (Digital imaging and computer vision series)*, 1st ed. CRC Press LLC, 2016.

[4] M. Emre Celebi, H. A. Kingravi, H. Iyatomi, Y. Alp Aslandogan, W. V Stoecker, R. H. Moss, J. M. Malters, J. M. Grichnik, A. A. Marghoob, H. S. Rabinovitz, and S. W. Menzies, "Border detection in dermoscopy images using statistical region merging," *Ski. Res. Technol.*, vol. 14, no. 3, pp. 347–353, 2008.

[5] C. Barata, M. Ruela, M. Francisco, T. Mendonça, and J. S. Marques, "Two Systems for the Detection of Melanomas in Dermoscopy Images Using Texture and Color Features," *IEEE Syst. J.*, pp. 1–15, 2013.

[6] M. E. Celebi, Q. Wen, S. Hwang, H. Iyatomi, and G. Schaefer, "Lesion Border Detection in Dermoscopy Images Using Ensembles of Thresholding Methods," *Ski. Res. Technol.*, vol. 19, no. 1, pp. e252–e58, Dec. 2013.

[7] K. Shimizu, H. Iyatomi, M. E. Celebi, K.-A. Norton, and M. Tanaka, "Four-class classification of skin lesions with task decomposition strategy.," *IEEE Trans. Biomed. Eng.*, vol. 62, no. 1, pp. 274–83, Jan. 2015.

[8] I. Maglogiannis, C. N. Doukas, and S. Member, "Overview of Advanced Computer Vision Systems for Skin Lesions Characterization," *IEEE Trans. Inf. Technol. Biomed.*, vol. 13, no. September, pp. 721–733, 2009.

[9] M. Silveira, J. C. Nascimento, J. S. Marques, A. R. S. Marçal, T. Mendonça, S. Yamauchi, J. Maeda, and J. Rozeira, "Comparison of segmentation methods for melanoma diagnosis in dermoscopy images," *Sel. Top. Signal Process. IEEE J.*, vol. 3, no. 1, pp. 35–45, 2009.

[10] T. Lee, V. Ng, R. Gallagher, A. Coldman, and D. McLean, "Dullrazor®: A software approach to hair removal from images," *Comput. Biol. Med.*, vol. 27, no. 6, pp. 533–543, Nov. 1997.

[11] A. Oppenheim, R. Schafer, and T. Stockham, "Nonlinear filtering of multiplied and convolved signals," *IEEE Trans. Audio Electroacoust.*, vol. 16, no. 3, pp. 437–466, 1968.

[12] R. Malladi, J. A. Sethian, and B. C. Vemuri, "Shape modeling with front propagation: A level set approach," *IEEE Trans. Pattern Anal. Mach. Intell.*, vol. 17, no. 2, pp. 158–175, 1995.

[13] N. Otsu, "A Threshold Selection Method from Gray-Level Histograms," *IEEE Trans. Syst. Man. Cybern.*, vol. 9, no. 1, pp. 62–66, 1979.

[14] J. a. Sethian, "Evolution, Implementation, and Application of Level Set and Fast Marching Methods for Advancing Fronts," *J. Comput. Phys.*, vol. 169, no. 2, pp. 503–555, May 2001.

[15] D. Gutman, N. C. F. Codella, E. Celebi, B. Helba, M. Marchetti, N. Mishra, and A. Halpern, "Skin Lesion Analysis toward Melanoma Detection: A Challenge at the International Symposium on Biomedical Imaging (ISBI) 2016, hosted by the International Skin Imaging Collaboration (ISIC)," *arXiv Prepr. arXiv1605.01397*, 2016.